



HAL
open science

Local nuclear magnetic resonance spectroscopy with giant magnetic resistance-based sensors

P. A. Guitard, R. Ayde, G. Jasmin-Lebras, L. Caruso, Myriam
Pannetier-Lecoeur, C. Fermon

► **To cite this version:**

P. A. Guitard, R. Ayde, G. Jasmin-Lebras, L. Caruso, Myriam Pannetier-Lecoeur, et al.. Local nuclear magnetic resonance spectroscopy with giant magnetic resistance-based sensors. Applied Physics Letters, 2016, 108, pp.212405. 10.1063/1.4952947 . cea-01485396

HAL Id: cea-01485396

<https://cea.hal.science/cea-01485396>

Submitted on 8 Mar 2017

HAL is a multi-disciplinary open access archive for the deposit and dissemination of scientific research documents, whether they are published or not. The documents may come from teaching and research institutions in France or abroad, or from public or private research centers.

L'archive ouverte pluridisciplinaire **HAL**, est destinée au dépôt et à la diffusion de documents scientifiques de niveau recherche, publiés ou non, émanant des établissements d'enseignement et de recherche français ou étrangers, des laboratoires publics ou privés.

Local nuclear magnetic resonance spectroscopy with giant magnetic resistance-based sensors

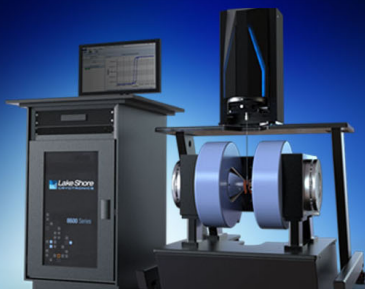
P. A. Guitard, R. Ayde, G. Jasmin-Lebras, L. Caruso, M. Pannetier-Lecoeur, and C. Fermon

Citation: *Appl. Phys. Lett.* **108**, 212405 (2016); doi: 10.1063/1.4952947

View online: <http://dx.doi.org/10.1063/1.4952947>


View Table of Contents: <http://aip.scitation.org/toc/apl/108/21>

Published by the [American Institute of Physics](#)



NEW 8600 Series VSM

For fast, highly sensitive
measurement performance

LEARN MORE 

Local nuclear magnetic resonance spectroscopy with giant magnetic resistance-based sensors

P. A. Guitard, R. Ayde,^{a)} G. Jasmin-Lebras, L. Caruso, M. Pannetier-Lecoecur, and C. Fermon

SPEC, CEA, CNRS, Université Paris-Saclay, CEA Saclay, 91191 Gif-sur-Yvette, France

(Received 14 March 2016; accepted 17 May 2016; published online 26 May 2016)

Nuclear Magnetic Resonance (NMR) spectroscopy on small volumes, either on microfluidic channels or *in vivo* configuration, is a present challenge. We report here a high resolution NMR spectroscopy on micron scale performed with Giant Magnetic Resistance-based sensors placed in a static magnetic B_0 field of 0.3 T. The sensing volume of the order of several tens of pL opens the way to high resolution spectroscopy on volumes unreached so far. *Published by AIP Publishing.*

[<http://dx.doi.org/10.1063/1.4952947>]

Nuclear Magnetic Resonance (NMR) spectroscopy is one of the most efficient techniques to study the structures or to determine the concentration of molecules. NMR spectroscopy using conventional micro-coils is limited to volumes between $10^6 \mu\text{m}^3$ (1 nL) and 1mm^3 ($1 \mu\text{L}$).¹⁻⁴ Recently, the use of single nitrogen-vacancy (NV) centers in diamond has been proposed to nanoscale resolution,⁵ but that approach is rather complicated. Our approach is based on micron size spin electronics based sensors, such as Giant Magnetic Resistance (GMR) and Tunnel Magnetic Resistance (TMR) for small volume detection. These sensors present a double advantage. First, they have flat field sensitivity up to GHz range.⁶ Second, these sensors can be easily implanted in the experimental set up just by placing it close enough to the region of interest. The only drawback compared to coils is the sensitivity to DC magnetic fields which requires specific sensor orientation to insure a proper detection.

The GMR sensor is integrated on a biocompatible substrate of silicon, glass, or sapphire which can be incorporated *in vivo* or *in vitro* like standard electrodes used for electrophysiology. It is patterned in a meander shape in a stack of the following composition:

Ta(5)/PtMn(18)/CoFe(2.3)/Ru(0.85)/CoFe(2.5)/Cu(2.9)/CoFe(1.5)/NiFe(3.5)/Ta(5)/SiO₂/Si.

The thicknesses are in nanometers. GMR's hard layer is a synthetic anti-ferromagnetic composed of PtMn/CoFe/Ru/CoFe. The spacer is a nonmagnetic layer of copper. The free layer is an association of CoFe with a soft ferromagnet NiFe having a magnetization that rotates easily with an external applied field (Figure 1). Tantalum constitutes the cap layer and the seed layer when it is, respectively, on the top and the bottom of the GMR. The meanders are made with $4 \mu\text{m}$ width lines and cover a rectangular surface with lateral sizes varying from $20 \mu\text{m}$ to $100 \mu\text{m}$. The extremities of the meander are short-circuited to avoid magnetic noise caused by domain formation. The magnetoresistance of the sensor without any applied magnetic field ($B_0=0\text{T}$) is about 6.4%/mT and a bias voltage of 5 V leads to a sensitivity of 320 V/T. As the NMR experiment is carried out in a main

field of 0.3 T, i.e., 13 MHz for the proton, then the sensor noise is not affected by the $1/f$ noise, but it is dominated by thermal noise of the sensor.⁷ The element resistance being 1 k Ω , the noise is $4.3 \text{nV}/\sqrt{\text{Hz}}$ which corresponds to a field equivalent noise of $12.5 \text{pT}/\sqrt{\text{Hz}}$.

GMR sensors are saturated by any in-plane field component larger than few mT. For that reason, the only way to perform NMR experiment in a polarizing field of few hundreds of mT with GMR sensors consists in applying the main field perfectly perpendicular to GMR's layer stack direction. In order to optimize the position of the GMR, our system is equipped with an angle adjustment for the GMR providing direction with accuracy better than 0.1° . Consequently, before starting the measurements, the adjustment of the sensor direction is made under an applied static magnetic field by measuring the GMR sensitivity to an external low frequency excitation.

The experimental set-up is presented in Fig. 2. In order to mimic an *in vivo* configuration, the sensor probe is simply inserted in a large liquid volume of 1.2cm^3 . A standard electromagnet has been used to generate a main field B_0 of about 0.3 T (13.3 MHz). In large perpendicular field, the free layer magnetization tends to get out of the plane, leading to a reduced projected component in the plane, and thus a decrease of sensitivity as can be seen in Fig. 3. At 0.3 T, GMR sensitivity reaches 5.3%/mT under 5 V bias voltage (Fig. 3) which corresponds to a sensitivity of 265 V/T. The excitation RF pulse is generated in a 1 cm diameter tuned coil. The RF pulse is applied along the Z direction during $40 \mu\text{s}$. Once the pulse is turned off, the Free Induction Decay (FID) signal is detected by the GMR sensor or by the same tuned coil for comparison. It should be noticed that, as the GMR is a broadband sensor, the recovery after RF excitation is fast and the ringing phenomena seen with tuned coil do not exist.

In that particular scheme, a direct coupling occurs between the GMR wire connections and the excitation/reception tuned coil. In order to separate the local GMR signal from the inductive signal, the GMR has been biased with an AC signal ω_m of few kHz. Thus, the signal of interest appears on both sides of the inductive signal shifted by the modulation current frequency ω_m .

^{a)} Author to whom correspondence should be addressed. Electronic mail: reina.ayde@cea.fr.

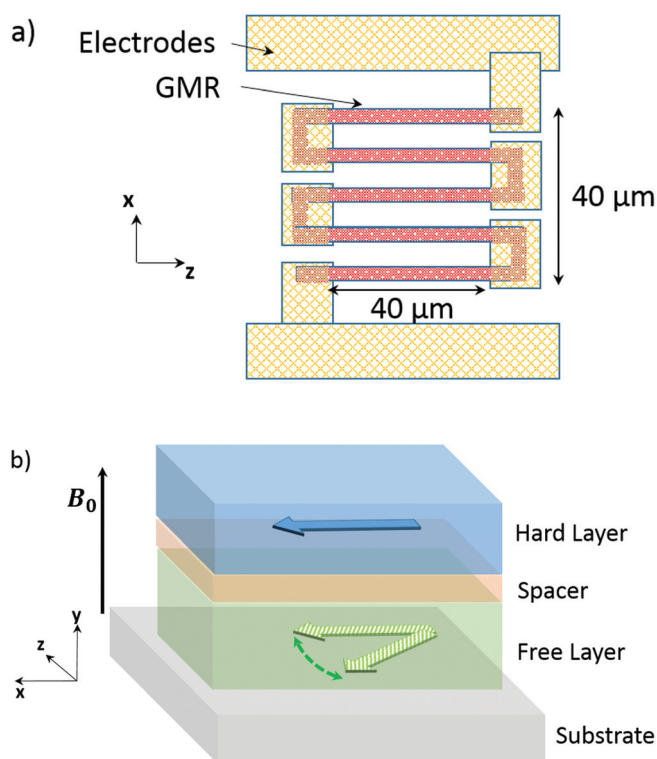


FIG. 1. (a) Top view schematic representation of the GMR meander geometry. The edges of the meander are short-circuited to avoid magnetic noise. (b) Cross section schematic representation of the GMR showing the different layers and their magnetizations.

The obtained modulated signal is amplified by a low noise preamplifier and split into two channels for quadrature detection. It is then demodulated and sent to an acquisition card. The sequence repetition time is 2 s.

Measurements were first performed on distilled water. We have measured the FID signal of water with a GMR probe, as shown in Fig. 4. The FFT of water FID signal detected for reference by the tuned coil for one acquisition

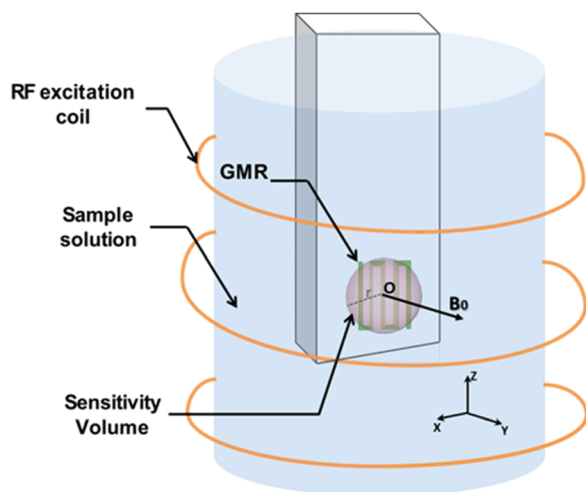


FIG. 2. Schematic representation of the experimental local NMR setup. The main field B_0 , generated by an electromagnet, is applied to the sample. An RF pulse is applied by a coil wound around the water sample at the corresponding Larmor frequency. The detection is done by the GMR sensor having a meander shape placed into a liquid solution. GMR sensor is sensitive to magnetic field in X direction.

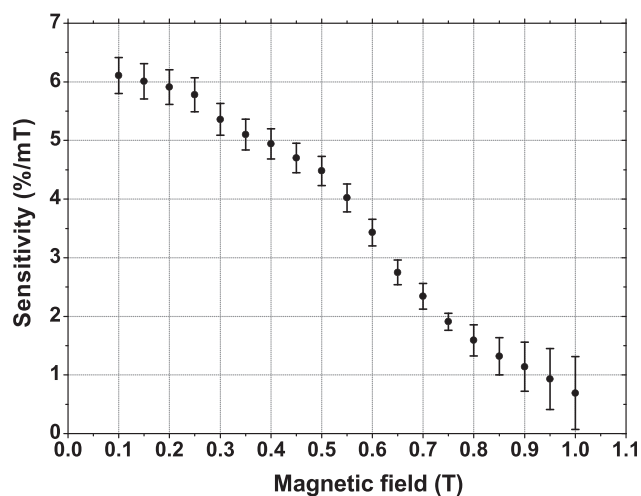


FIG. 3. Sensitivity of a GMR decreases when a magnetic field perpendicular to the stack direction is applied. This is explained by the interaction of the free layer magnetization with B_0 , which tends to move out of the stack plane, therefore decreasing GMR sensitivity. Since the sensitivity decreases when the applied field increases, the error is considered as an exponential function.

has a linewidth of about 14 Hz which corresponds to 1 ppm field homogeneity and a time constant $T_2^* \sim 70$ ms.

The signal is modulated at 3 kHz via an AC voltage of 5 V applied to the GMR. As we cannot detect the signal with only 1 acquisition, the linewidth of the GMR signal is not given by the spatial homogeneity which is very good on Nano Liters volumes but by the stability in time of the field which is about 1 ppm/h. Hence, we used the signal of tuned coil as a signal lock of main field changes implying a comparable linewidth for GMR detected signal and tuned coil detected signal. Regarding sensitivity, an averaging of 400 acquisitions was required to get a signal-to-noise ratio (SNR) of 3. The SNR value is determined from the amplitude of FFT signal and the standard deviation of the noise in Fig. 4.

In order to estimate the volume, the GMR element is sensing, and to verify the experimental results, we computed, first, the magnitude of the total magnetic field flux B induced

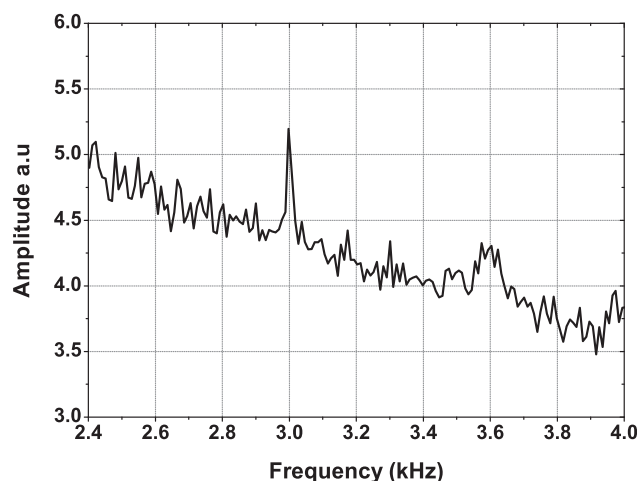


FIG. 4. FFT of water FID spectrum detected by the GMR in 400 acquisitions. The SNR is 3. The signal is modulated by a 3 kHz AC voltage. Decreasing slope is due to additional noise caused by tuned coil coupled inductively to the GMR.

by a semi-spherical volume of water solution having a radius r and centered at O (O is considered as a point at the center of the sensor). Computation is done at $t=0$ s after turning off the RF excitation applied along the Z direction. The water volume was discretized in a set of small cubes having a unitary volume of $1 \mu\text{m}^3$ and a magnetization at $t_0 = 0$ s of⁸

$$\vec{m}(t_0) = \frac{N_0 \gamma^2 \left(\frac{h}{2\pi}\right)^2 I(I+1) B_0}{3k_B T} V_s \vec{k}, \quad (1)$$

where N_0 is the number of protons in a volume unit, γ is the gyromagnetic factor, h is the Planck's constant, I is the quantum spin number, k_B is the Boltzman constant, T is the temperature in Kelvin, V_s is the volume, and \vec{k} is the unit vector of Z axis.

The magnetic field flux induced at O is the sum of the magnetic contribution of each dipole on this point, and it is given by

$$B(t_0) = \sum_i \frac{\mu_0}{4\pi} \left(\frac{3\vec{r}(\vec{m}_i \cdot \vec{r})}{r^5} - \frac{\vec{m}_i}{r^3} \right), \quad (2)$$

where \vec{r} is the distance between a dipole and O , and μ_0 is the vacuum permeability.

Fig. 5 presents the magnitude of $B(t_0)$ as a function of the radius of a semi-spherical volume of water detected in one point. It can be inferred that 95% of the magnetic flux detected by a punctual GMR is due to a semi-spherical volume of $15 \mu\text{m}$ radius. Accordingly, GMR elements are mostly sensitive to the very close dipoles. Then, the total volume contributing in GMR signal can be constructed by convoluting this semi spherical volume through GMR surface. Thus, the total volume of sensibility for the used GMR of $40 \times 40 \mu\text{m}^2$ surface is a rounded volume of $70 \times 70 \times 15 \mu\text{m}^3$ which corresponds to 62 pL. This result shows the relevancy of employing GMR sensors for local NMR application. In addition, that simulation shows that in that configuration, the minimum volume which can be sensed will be given by a half sphere of $15 \mu\text{m}$ of radius which corresponds to 2 pL.

Since the induced magnetic field $B(t_0)$ is related to the area under the Fast Fourier Transform (FFT) peak of a FID by the equation: $B(t_0) = \frac{1}{\sqrt{2\pi}} \int S(\omega) d\omega$, the amplitude of the NMR frequency spectrum, S_0 , can be calculated:

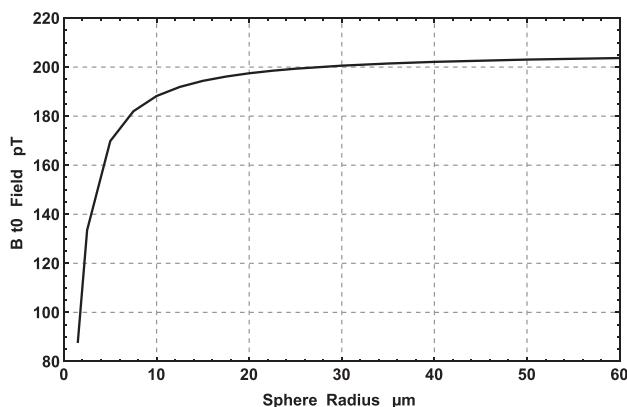


FIG. 5. Total magnetic field induced by a semi spherical volume on its center as a function of its radius.

$S_0 \sim \frac{2\sqrt{2}B(t_0)}{\Delta\omega\sqrt{\pi}} \sim 22 \text{ pT}$, with $\Delta\omega \sim 14 \text{ Hz}$ being the Full Width of Half Maximum of the peak. On the other hand, as discretization is of 10 Hz, the amplitude of GMR Root Mean Square (RMS) noise is about 40 pT. Consequently, we expect that 30 acquisitions will at least be required to obtain a SNR of 3. Indeed, the required number of acquisitions in the experiment was higher. This is due to the additional noise caused by the tuned coil which couples inductively to the GMR. This appears in Fig. 4, by a decreasing slope.

In order to compare the performance of GMR to an inductive microcoil, we considered the results reported by McDowell and Adolphi⁴ obtained with one of the smallest solenoid inductive microprobe: a SNR of $0.46/\sqrt{\text{Hz}}$ was achieved on a sample volume of 1.2 nL at 1 T with one acquisition. Since SNR is given by⁹

$$\text{SNR} \propto V_s \omega_0^{7/4}. \quad (3)$$

SNR of the microprobe will be 160 times less for a volume of 62 pL at 0.3 T. This is equivalent to 1.1×10^5 acquisitions to get a SNR of 3. Thus, GMRs are much more efficient than micro-probes for NMR measurements of pL volumes at low magnetic field.

Furthermore, measurements were also performed on ethanol. Protons of ethanol ($\text{CH}_3\text{-CH}_2\text{-OH}$) have three

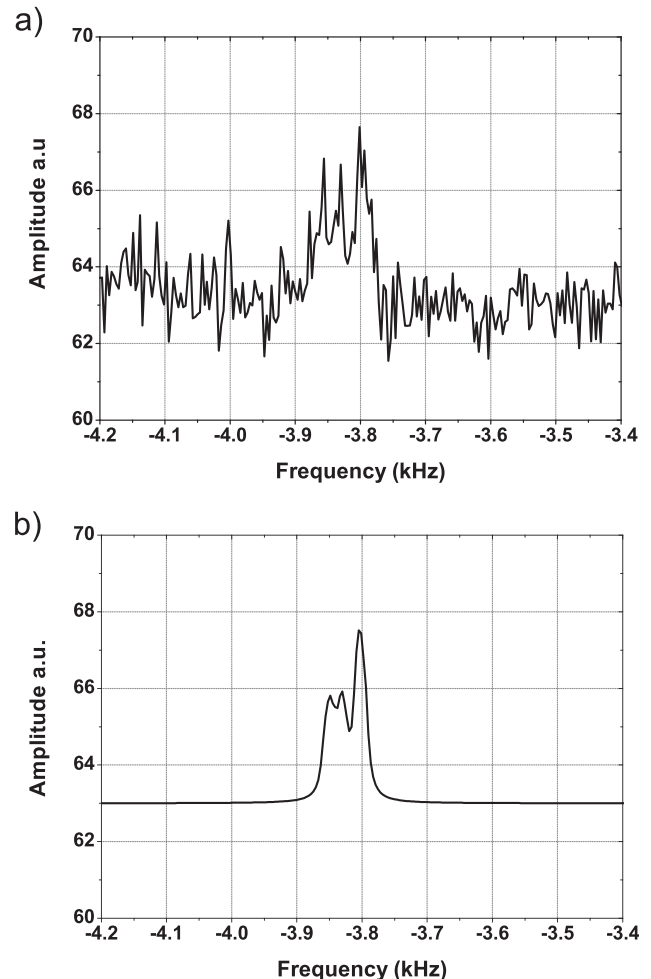


FIG. 6. (a) Experimental NMR spectrum of ethanol detected by GMR sensor over 3000 averaging. (b) Simulated NMR spectrum of ethanol at 0.3 T.

different chemical environments corresponding to three different chemical shifts. Fig. 6 presents the spectrum of ethanol detected with the GMR sensor obtained in 3000 acquisitions. As with water solution, modulation signal is of 5 V and has a frequency of 3.8 kHz. Obtained SNR is about 3. Furthermore, NMR peaks of ethanol with the corresponding chemical shift¹⁰ were simulated using SpinDynamica code for Wolfram Mathematica¹¹ at 0.3 T and were compared to experimental results. A good agreement of chemical shifts between experimental and theoretical results is observed.

We have shown the capacity of a GMR sensor to perform local NMR spectroscopy. This sensor takes advantage of having high sensitivity and a large bandwidth, working at room temperature and practical to be applied on small *in vivo* volume or on a microfluidic channels.

First, local performance of GMR was shown by estimating its volume resolution. Taking into account that this volume depends on the GMR surface, a volume resolution less than 62 pL could be reached. Then, the feasibility of NMR acquisition on water and ethanol was demonstrated with a SNR of 3 in 400 and 3000 acquisitions for water and ethanol, respectively, while maintaining acceptable resolution capacity of 1 ppm.

Furthermore, we believe that the reachable SNR is higher than presented experimental results because of the inductively coupled noise of excitation coil. Thus, the next step will focus on how to get rid of inductive coupling.

Future steps will concentrate on improving resolution capability by adjusting the spatial and temporal homogeneity

of the static field which is now the main experimental limitation. Moreover, in order to get better sensitivity, a different kind of magnetoresistive devices could be studied: Magnetic Tunneling Junctions (MTJ).¹² Indeed, this device has sensitivity 10 times better than that of a GMR, which practically means, to get the same SNR, TMR requires 100 acquisitions averaging less than GMR.

We acknowledge Patrick Berthault for the calculation of the Ethanol spectrum at 0.3 T and also the European Commission for its support through the FET initiative Magnetron, FP7-ICT-2011- project 600730.

¹H. Lee, E. Sun, D. Ham, and R. Weissleder, *Nat. Med.* **14**, 869 (2008).

²A. P. M. Kentgens, J. Bart, P. J. M. van Bentum, A. Brinkmann, E. R. H. van Eck, J. G. E. Gardeniers, J. W. G. Janssen, P. Knijn, S. Vasa, and M. H. W. Verkuijlen, *J. Chem. Phys.* **128**, 052202 (2008).

³A. G. Webb, *J. Magn. Reson.* **229**, 55 (2013).

⁴A. McDowell and N. Adolphi, *J. Magn. Reson.* **188**, 74 (2007).

⁵S. DeVience, L. Pham, I. Lovchinsky, A. Sushkov, N. Bar-Gill, C. Belthangady, F. Casola, M. Corbett, H. Zhang, M. Lukin, H. Park, A. Yacoby, and R. Walsworth, *Nat. Nanotechnol.* **10**, 129 (2015).

⁶R. Ko and M. Blodgett, *Rev. Quant. Nondestr. Eval.* **22**, 844 (2003).

⁷M. Pannetier, C. Fermon, G. Le Goff, J. Simola, E. Kerr, and J. M. D. Coey, *J. Magn. Magn. Mater.* **290**, 1158 (2005).

⁸A. Abragam, *The Principles of Nuclear Magnetism* (Presses Universitaire de France, 1961), p 2.

⁹D. I. Hoult and R. E. Richards, *J. Magn. Reson.* **24**, 71 (1976).

¹⁰H. Gottlieb, V. Kotlyar, and A. Nudelman, *J. Org. Chem.* **62**, 7512 (1997).

¹¹M. H. Levitt, J. Rantaharju, and A. Brinkmann, SpinDynamica code for Wolfram Mathematica, see www.SpinDynamica.soton.ac.uk.

¹²T. Miyazaki and N. Tezuka, *J. Magn. Magn. Mater.* **139**, 231 (1995).